International Journal of Engineering Science 47 (2009) 512–523

Contents lists available at ScienceDirect

International Journal of Engineering Science

journal homepage: www.elsevier.com/locate/ijengsci

Modal power flow with application to damage detection

X.Q. Wang *,[1], W.O. Wong, L. Cheng

Department of Mechanical Engineering, The Hong Kong Polytechnic University, Hung Hom, Kowloon, Hong Kong SAR, PR China

ARTICLE INFO

Article history:
Received 15 November 2007
Received in revised form 2 July 2008
Accepted 22 August 2008
Available online 14 October 2008

Keywords:
Modal power flow
Damage detection

ABSTRACT

Features of power flow of an undamped beam at resonance are studied in the present paper. It is found that when an undamped beam undergoes free vibration at one of its natural frequencies, the active component of the power flow becomes zero while the reactive component is of modal pattern, whose characteristic frequency is twice of the natural frequency. The power flow in this case can thus be termed as modal power flow. The instantaneous energy density associated with the vibration mode consists of a static component and a dynamic component, related to the mean total and Lagrangian energy densities, respectively. The modal power flow is relevant to the latter but independent of the former. Potential application of modal power flow to structural damage detection is investigated. Two typical damages, transverse cracks and delaminations, are considered. A damage index based on the modal power flow is proposed, and compared with the damage indices based on the slope, the bending strain, and the strain energy through numerical examples. The imperfection of boundary conditions is also considered. It is shown that the proposed damage index is sensitive to both types of damage, thus can be used as an universal damage indicator.

1. Introduction

The concept of structural intensity has been extensively used to understand the transmission of mechanical energy through an elastic body undergoing oscillatory motion. For a three-dimensional elastic body in the Cartesian coordinate system, the structural intensity of a particle located at the position $\{x, y, z\}$ is expressed as [1]

$$\mathbf{I}(x,y,z,t) = I_x(x,y,z,t)\vec{i} + I_y(x,y,z,t)\vec{j} + I_z(x,y,z,t)\vec{k}, \tag{1}$$

where

$$I_x = -\sigma_{xx}\dot{u}_x - \tau_{xy}\dot{u}_y - \tau_{xz}\dot{u}_z, \tag{2a}$$
$$I_y = -\tau_{yx}\dot{u}_x - \sigma_{yy}\dot{u}_y - \tau_{yz}\dot{u}_z, \tag{2b}$$
$$I_z = -\tau_{zx}\dot{u}_x - \tau_{zy}\dot{u}_y - \sigma_{zz}\dot{u}_z. \tag{2c}$$

In the above expression, σ and τ are dynamic normal and shear stresses, respectively, and u is the particle displacements at the observation point, their subscripts representing component orientation. From the definition, it can be seen that the components of structural intensity are the products of stresses and particle velocities, having dimensions of power per unit area.

For practical structural members such as beams, structural intensity is usually expressed as the integration of Eq. (1) across the cross-sectional area of the member, then structural intensity actually describes the energy transmitted through

* Corresponding author. Tel.: +1 602 314 0630.
E-mail address: julianxqwang@hotmail.com (X.Q. Wang).
[1] Department of Mechanical and Aerospace Engineering, Arizona State University, Tempe, AZ 85287, USA.

0020-7225/$ - see front matter © 2008 Elsevier Ltd. All rights reserved.
doi:10.1016/j.ijengsci.2008.08.007

the area, and its unit becomes that of the power. Hence, the term 'power flow' is more suitable for the description of structural intensity in practical structural members.

Since the introduction of the concept of power flow, its computation and measurement have received great attention due to its importance in locating vibration sources and sinks and identifying vibration propagating paths [2]. In the computational aspect, the formulae for simple structural members are available as summarized by Pavic [1]. For structures of complex geometries, finite element method (FEM) can be used [3]. The concept of power flow has also been used in vibro-acoustic analysis of complex structures in the mid- and the high-frequency ranges [4,5], as an alternative approach to the classical statistical energy method (SEM). The measurement of power flow was firstly addressed by Noiseux [6] for uniform beams and plates, by analogy with acoustic intensity. The key problem is to determine spatial derivatives of structural motions obtained by either contacting or non-contacting techniques, in order to evaluate the power flow. A commonly used method is the finite difference scheme introduced by Pavic [7]. However, the error induced by the finite difference approximation becomes large for high-order derivatives. Therefore, other methods have been proposed, e.g., the wave component approach [8], the wave number processing technique [9], etc.

Since power flow is a direct measure of energy transmission through the structure, it has also been used as a cost function in active control. Schwenk et al. [10] demonstrated that the effectiveness of controlling power flow depends on the relative location of the error sensor and the control actuator, and it is also limited by the accuracy of the measurement. By taking the evanescent waves into the control algorithm, Audrain et al. [11] showed that controlling power flow is particularly effective when the distance between the sensor and the actuator is smaller than a structural wavelength.

In recent years, the concept of power flow has also been applied to structural damage detection. Using the finite element method, Khun et al. [12] studied the power flow pattern of a plate with single or multiple cutouts. It was found that the magnitude of power flow experiences significant change near the cutout boundary. Lee et al. [13] further showed that this feature can be used to locate the crack. For beam and shell structures, Zhu et al. [14,15] showed that the characteristics of the power flow passing through a crack are relevant to its location and its depth, thus can be used to identify the crack.

In all these studies, the power flow was studied from the point of view of propagating wave. For the purpose of damage detection, however, the vibration mode shape and its relevant entities, e.g., its curvature (bending strain) [16,17], and the strain energy associated with the mode [18], have been commonly used as the indicators of damage. For a comprehensive review of these mode-relevant damage indicators, the readers are referred to Refs. [19,20].

In the present study, the features of power flow associated with a vibration mode of both intact and damaged beams are investigated, in attempt to develop a novel damage indicator and the associated damage index. In the present paper, the damage indicator refers to the physical damage-sensitive entity, while the damage index is a function of the damage indicator which gives a quantitative measure of the variation of the damage indicator with the damage. The damage index can be simply a nondimensionalization or a normalization of the damage indicator, or a complex function of the damage indicator obtained from advanced signal processing. It will be shown that, when the damping is assumed small hence negligible, the reactive component of power flow is relevant to the mean Lagrangian energy density associated with the corresponding vibration mode, while the active component is zero. The effect of damage on the reactive power flow associated with a vibration mode is demonstrated by several numerical examples, and its potential as a universal damage indicator is shown. Beams are used in the examples, but the approach can be extended to plates and shells. The imperfection of boundary conditions is taken into account by considering that the beam is elastically supported at two ends.

2. Reactive power flow of a beam at resonance

Consider an undamped beam shown in Fig. 1. According to Timoshenko beam theory, the stress field at a cross section of the beam is given by

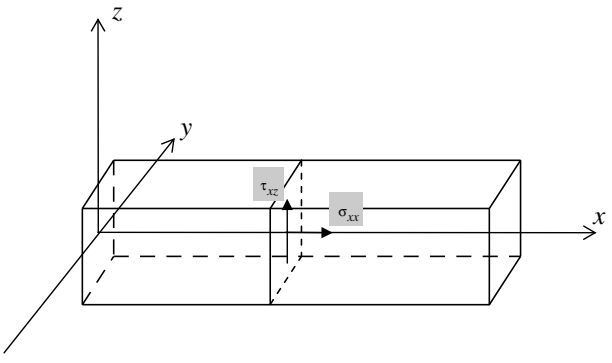

Fig. 1. Illustration of a beam and its stress field in cross section.

$$\sigma_{xx} = E \cdot \varepsilon_{xx}, \tag{3a}$$
$$\tau_{xz} = \kappa G \gamma_{xz}, \tag{3b}$$

where σ and τ are normal and shear stresses, ε and γ are normal and shear strains, and E and G are Young's modulus and shear modulus, respectively. κ is the shear coefficient.

The strain–displacement relationship is given by

$$\varepsilon_{xx} = \frac{\partial(\phi \cdot z)}{\partial x} = z\frac{\partial \phi}{\partial x}, \tag{4a}$$
$$\gamma_{xz} = \frac{\partial w}{\partial x} - \phi, \tag{4b}$$

where w and ϕ are translational displacement and bending rotation of the beam element, respectively.

For a beam, the expression of structural intensity is reduced to one dimensional, written as

$$\mathbf{I} = I_x \vec{i}, \tag{5}$$

where

$$I_x = -\sigma_{xx}\dot{u} - \tau_{xz}\dot{w}. \tag{6}$$

Substituting Eqs. (3a), (3b), (4a), and (4b) into Eq. (6), and integrating across the cross section, A, one obtains,

$$P_x \equiv \int_A I_x \mathrm{d}A = \int_A (-\sigma_{xx}\dot{u} - \tau_{xz}\dot{w})\mathrm{d}A = -EI\frac{\partial \phi}{\partial x} \cdot \dot{\phi} - \kappa GA\left(\frac{\partial w}{\partial x} - \phi\right) \cdot \dot{w} \tag{7}$$

where I is the second moment of area of the cross section about the neutral line.

Eq. (7) can be applied to either a propagating wave or a standing wave (a mode of vibration). For the nth mode of the beam, its motion can be described by

$$\left\{ \begin{matrix} w(x,t) \\ \phi(x,t) \end{matrix} \right\} = \left\{ \begin{matrix} W_n(x) \\ \Phi_n(x) \end{matrix} \right\} \sin \omega_n t, \quad n = 1, 2, 3, \ldots, \tag{8}$$

where $\omega_n = 2\pi f_n$; f_n the natural frequency of the mode and $\left\{ \begin{matrix} W_n(x) \\ \Phi_n(x) \end{matrix} \right\}$ the vector of corresponding mode shapes.

For this mode, the power flow is written as

$$\mathbf{P}(x,t) = P_x(x,t)\vec{i}, \tag{9}$$

where

$$\begin{aligned} P_x(x,t) &= -\left[KGA\left(\frac{\partial w}{\partial x} - \phi\right) \cdot \dot{w} + EI\frac{\partial \phi}{\partial x} \cdot \dot{\phi}\right] \\ &= -\frac{1}{2}\omega_n\left\{\kappa GA\left[\frac{\mathrm{d}W_n(x)}{\mathrm{d}x} - \Phi_n(x)\right] \cdot W_n(x) + EI\frac{\mathrm{d}\Phi_n(x)}{\mathrm{d}x} \cdot \Phi_n(x)\right\} \cdot \sin 2\omega_n t = -P_n(x)\sin 2\omega_n t. \end{aligned} \tag{10}$$

It can be seen that the active component of the power flow is zero for an undamped beam vibrating at one of its natural frequencies, hence the power flow associated with a mode actually represents the reactive energy, which is expressed in the form of a mode at a characteristic frequency $2\omega_n$. $P_n(x)$ can thus be defined as the modal power flow of the beam corresponding to the natural frequency ω_n, expressed as

$$P_n(x) = \frac{1}{2}\omega_n\left\{\kappa GA\left[\frac{\mathrm{d}W_n(x)}{\mathrm{d}x} - \Phi_n(x)\right] \cdot W_n(x) + EI\frac{\mathrm{d}\Phi_n(x)}{\mathrm{d}x} \cdot \Phi_n(x)\right\}. \tag{11}$$

3. Features of modal power flow

Structural intensity represents the instantaneous power (rate of energy) transmission at an infinitesimal volume of a general elastic body. For practical structural members, structural intensity is in the form of power flow, which consists of two components in general; one is called the active component representing the power passing through without returning, and the other is called the reactive component representing the power fluctuating back and forth with zero mean value.

When an undamped structural member is finite, it has an infinite number of vibration modes; the active component of its power flow associated with one of these modes becomes zero, and the reactive component appears in the modal form whose characteristic frequency is the double of the modal frequency. This modal power flow represents a pattern of reactive power distribution across the structural member for the corresponding mode of vibration. It is thus expected that the modal power flow is relevant to the energy distribution of the structural member vibrating at that mode. This is studied in the following in favor of further physical understanding.

According to Timoshenko beam theory, the kinetic and the potential energies are expressed as, respectively,

$$T(t)=\frac{1}{2}\int_0^L\left\{m\left[\frac{\partial w(x,t)}{\partial t}\right]^2+J\left[\frac{\partial\phi(x,t)}{\partial t}\right]^2\right\}\mathrm{d}x, \tag{12a}$$

$$V(t)=\frac{1}{2}\int_0^L\left\{EI\left[\frac{\partial^2\phi(x,t)}{\partial x^2}\right]^2+\kappa GA\left[\frac{\partial w(x,t)}{\partial x}-\phi(x,t)\right]^2\right\}\mathrm{d}x. \tag{12b}$$

where $m=\rho A$, and $J=\rho I$, ρ is the density of beam material.

For an infinitesimal beam element of length Δx located at the position x, the instantaneous total energy is given by

$$\begin{aligned}\Delta E(x,t)&=\Delta T(x,t)+\Delta V(x,t)\\&=\frac{1}{2}\left\{m\left[\frac{\partial w(x,t)}{\partial t}\right]^2+J\left[\frac{\partial\phi(x,t)}{\partial t}\right]^2\right\}\Delta x+\frac{1}{2}\left\{EI\left[\frac{\partial\phi(x,t)}{\partial x}\right]^2+\kappa GA\left[\frac{\partial w(x,t)}{\partial x}-\phi(x,t)\right]^2\right\}\Delta x.\end{aligned} \tag{13}$$

The energy density of a beam is defined as

$$e(x,t)=\lim_{\Delta x\to 0}\frac{\Delta E(x,t)}{\Delta x}=\frac{1}{2}\left\{\left(m\left[\frac{\partial w(x,t)}{\partial t}\right]^2+J\left[\frac{\partial\phi(x,t)}{\partial t}\right]^2\right)+\left(EI\left[\frac{\partial\phi(x,t)}{\partial x}\right]^2+\kappa GA\left[\frac{\partial w(x,t)}{\partial x}-\phi(x,t)\right]^2\right)\right\}. \tag{14}$$

The time derivative of the energy density reads

$$\frac{\partial e(x,t)}{\partial t}=\left\{m\dot{w}(x,t)\ddot{w}(x,t)+J\dot{\phi}(x,t)\ddot{\phi}(x,t)+EI\left[\frac{\partial\phi(x,t)}{\partial x}\right]\left[\frac{\partial\dot{\phi}(x,t)}{\partial x}\right]+\kappa GA\left[\frac{\partial w(x,t)}{\partial x}-\phi(x,t)\right]\left[\frac{\partial\dot{w}(x,t)}{\partial x}-\dot{\phi}(x,t)\right]\right\}. \tag{15}$$

Noting that

$$m\ddot{w}(x,t)=\kappa GA\left[\frac{\partial^2 w(x,t)}{\partial x^2}-\frac{\partial\phi(x,t)}{\partial x}\right], \tag{16a}$$

$$J\ddot{\phi}(x,t)=EI\frac{\partial^2\phi(x,t)}{\partial x^2}+\kappa GA\left[\frac{\partial w(x,t)}{\partial x}-\phi(x,t)\right], \tag{16b}$$

one obtains,

$$\begin{aligned}\frac{\partial e(x,t)}{\partial t}&=\left\{\kappa GA\left[\frac{\partial^2 w(x,t)}{\partial x^2}-\frac{\partial\phi(x,t)}{\partial x}\right]\dot{w}(x,t)+\kappa GA\left[\frac{\partial w(x,t)}{\partial x}-\phi(x,t)\right]\frac{\partial\dot{w}(x,t)}{\partial x}\right\}\\&\quad+\left\{EI\left[\frac{\partial^2\phi(x,t)}{\partial x^2}\right]\dot{\phi}(x,t)+EI\left[\frac{\partial\phi(x,t)}{\partial x}\right]\left[\frac{\partial\dot{\phi}(x,t)}{\partial x}\right]\right\}\\&=\kappa GA\frac{\partial}{\partial x}\left\{\left[\frac{\partial w(x,t)}{\partial x}-\phi(x,t)\right]\dot{w}(x,t)\right\}+EI\frac{\partial}{\partial x}\left\{\left[\frac{\partial\phi(x,t)}{\partial x}\right]\dot{\phi}(x,t)\right\}\\&=\frac{\partial}{\partial x}\left\{\kappa GA\left[\frac{\partial w(x,t)}{\partial x}-\phi(x,t)\right]\dot{w}(x,t)+EI\left[\frac{\partial\phi(x,t)}{\partial x}\right]\dot{\phi}(x,t)\right\}\end{aligned} \tag{17}$$

Compared with the expression of the power mode, Eq. (10), it can be seen that

$$\frac{\partial e(x,t)}{\partial t}=-\frac{\partial P_x(x,t)}{\partial x}. \tag{18}$$

Eq. (18) gives the relationship between power flow and energy density of the beam. Physically, this represents the energy balance of a beam element under free vibration, as illustrated in Fig. 2. In Fig. 2, an infinitesimal beam element located at $x=x_i$ and of the length $\Delta x=x_{i+1}-x_i$ is highlighted. The energy of this element is $\Delta E=e(x_i,t)\cdot\Delta x$. The terms $P_x(x_i,t)$ and $P_x(x_{i+1},$

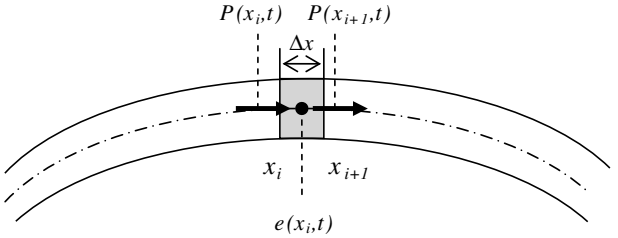

Fig. 2. Illustration of the relationship between power flow and energy density for an infinitesimal beam element under free vibration.

t) represent the power passing through its two ends at $x = x_i$ and $x = x_{i+1}$, respectively. The energy balance of the element, within a infinitesimal period of time, Δt, is written as

$$P_x(x_i,t)\cdot\Delta t = [e(x_i,t+\Delta t) - e(x_i,t)]\cdot\Delta x + P_x(x_{i+1},t)\cdot\Delta t. \tag{19}$$

After some mathematical manipulation, one obtains,

$$\frac{e(x_i,t+\Delta t)-e(x_i,t)}{\Delta t} = -\frac{P_x(x_{i+1},t)-P_x(x_i,t)}{\Delta x}. \tag{20}$$

Taking the limit of Eq. (20) for $\Delta x \to 0$ and $\Delta t \to 0$, one obtains Eq. (18).

Eq. (18) is applicable to both a propagating wave and a vibration mode (standing wave), while the latter is concerned in the present study. When a beam vibrates at one of its natural frequencies, its motion is given by $\begin{Bmatrix} w(x,t) \\ \phi(x,t) \end{Bmatrix} = \begin{Bmatrix} W_n(x) \\ \Phi_n(x) \end{Bmatrix} \sin\omega_n t$ where n is the mode number, and the energy density is expressed as

$$\begin{aligned} e_n(x,t) &= \frac{1}{4}\left\{\omega_n^2\left[mW_n^2(x)+J\Phi_n^2(x)\right] + \left[EI\left(\frac{d\Phi_n(x)}{dx}\right)^2 + \kappa GA\left(\frac{dW_n(x)}{dx}-\Phi_n(x)\right)^2\right]\right\} \\ &\quad + \frac{1}{4}\left\{\omega_n^2\left[mW_n^2(x)+J\Phi_n^2(x)\right] - \left[EI\left(\frac{d\Phi_n(x)}{dx}\right)^2 + \kappa GA\left(\frac{dW_n(x)}{dx}-\Phi_n(x)\right)^2\right]\right\}(\cos 2\omega_n t) \\ &= E_n(x) + L_n(x)\cos 2\omega_n t \end{aligned} \tag{21}$$

where

$$E_n(x) = \frac{1}{4}\left\{\omega_n^2\left[mW_n^2(x)+J\Phi_n^2(x)\right] + \left[EI\left(\frac{d\Phi_n(x)}{dx}\right)^2 + \kappa GA\left(\frac{dW_n(x)}{dx}-\Phi_n(x)\right)^2\right]\right\},$$

$$L_n(x) = \frac{1}{4}\left\{\omega_n^2\left[mW_n^2(x)+J\Phi_n^2(x)\right] - \left[EI\left(\frac{d\Phi_n(x)}{dx}\right)^2 + \kappa GA\left(\frac{dW_n(x)}{dx}-\Phi_n(x)\right)^2\right]\right\}.$$

From Eq. (21), it can be seen that the energy density for a mode of the beam consists of two components. One is a static component, $E_n(x)$, and the other is a dynamic component, $L_n(x)\cos 2\omega_n t$. At any instant, the energy density of the beam is the superposition of these two components.

The static component, $E_n(x)$, is actually the mean total energy density, whose integration along the beam gives the total energy of the beam corresponding to the mode. The amplitude of the dynamic component, $L_n(x)$, on the other hand, represents the mean Lagrangian energy density associated with the mode.

The dynamic component, $L_n(x)\cos 2\omega_n t$, implies that there exists instantaneous energy exchange between adjacent beam elements during one period of vibration. The static component, $E_n(x)$, is not involved in this energy exchange. The power mode, $P_n(x)$, is related to the dynamic component only, and the relationship can be obtained by substituting Eq. (21) into Eq. (18), yielding

$$\frac{dP_n(x)}{dx} = -(2\omega_n)L_n(x). \tag{22}$$

In practice, modal power flow of a structure can be determined by the spatial distribution of the amplitude of the steady reactive power flow in the structure when it is excited at this natural frequency. Various techniques proposed for the measurement of power flow, e.g., the finite difference scheme [7] and the wave component approach [8], can be used.

4. Application of modal power flow to damage detection

From the expression of the modal power flow, it can be seen that it is a combination of several other modal parameters including the natural frequency, the displacement, the slope, the curvature (bending strain), and the shear strain mode shapes. It is well known that the damage in the structure would alter these modal parameters, locally or globally. Some of these modal parameters, such as the natural frequency, the displacement and the strain mode shapes, have been used in damage detection. However, the individual mode shape may be sensitive to certain type of damage only, and the sensitivity is low at nodal points of the mode shape. The modal power flow, as a combination of the modal parameters, is expected to be an indicator of such damage. In the following, the sensitivity of the modal power flow to the damage will be analyzed. The beam is considered in the analysis, but the conclusions drawn can be extended to the plate and the shell.

4.1. Damage index based on modal power flow

In many practical cases, the structures are slender or thin, thus the effects of rotary inertia and shear deformation are not significant. Simplified formulae for the modal power flow are thus sufficient, and this would also simplify the measurement of modal power flow.

Table 1
List of the boundary conditions used in numerical examples

	K_L	T_L	K_R	T_R
Cantilever	10^{20}	10^{20}	0	0
Simply-supported	10^{20}	0	10^{20}	0
Elastic support (a)	10^{20}	10^{20}	10^{20}	10^{7}
Elastic support (b)	10^{20}	10^{20}	10^{7}	10^{20}
Elastic support (c)	10^{20}	10^{20}	10^{7}	10^{7}

The expression of modal power flow for a beam, Eq. (11), can be rewritten as

$$P_n(x) = \frac{1}{2}\omega_n[Q_n(x)\cdot W_n(x) + M_n(x)\cdot \Phi_n(x)]. \tag{23}$$

where $Q_n(x)$ and $M_n(x)$ are the shear force and the bending moment, respectively.

When the rotary inertia and shear deformation are negligible, according to Euler beam theory, $\Phi_n(x) = W_n'(x), M_n(x) = EIW_n''(x)$, and $Q_n(x) = -EIW_n'''(x)$, a simplified formula of the modal power flow can be written as

$$P_n(x) = \frac{1}{2}\omega_n D_E\left[W_n''(x)W_n'(x) - W_n'''(x)W_n(x)\right], \tag{24}$$

where $D_E = EI$ is the bending stiffness. Using the simplified formulae, a damage index based on the modal power flow is developed in the following.

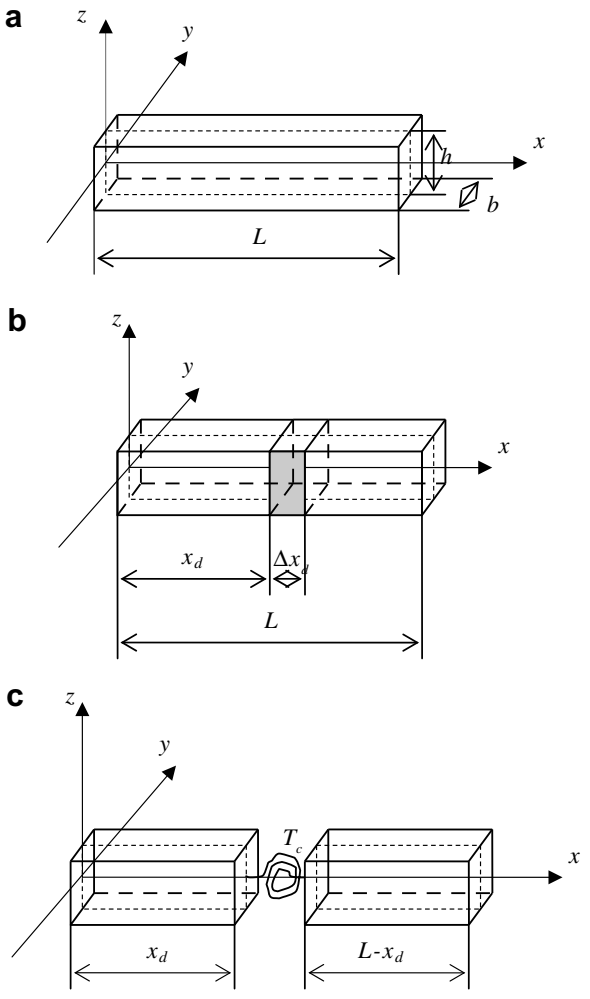

Fig. 3. Examples of damaged structures. (a) Intact beam; (b) delaminated beam and (c) model of cracked beam.

Consider the case that there is a damage of length Δx_d at the location $x = x_d$ of a beam, while the beam is intact otherwise. Usually, the damage induces a local change of the stiffness of the beam, which can be expressed as

$$\widetilde{D}_E = D_E[1 + \varepsilon_E \tilde{u}(\Delta x_d)], \tag{25}$$

where the overhead '$\sim$' represents the quantity of a damaged beam, and ε_E represents the percentage change of D_E due to the damage. The function $\hat{u}(\Delta x_d)$ is defined as

$$\hat{u}(\Delta x_d) = u(x - x_d) - u[(x - (x_d + \Delta x_d))], \tag{26}$$

where $u(x)$ is the unit step function.

For such a damaged beam, the modal power flow is expressed as

$$\widetilde{P}_n(x) = \frac{1}{2}\tilde{\omega}_n \widetilde{D}_E \left\{ \widetilde{W}_n'''(x) \cdot \widetilde{W}_n(x) - \widetilde{W}_n''(x) \cdot \widetilde{W}_n'(x) \right\}. \tag{27}$$

The change of natural frequency due to damage is global, thus does not contribute to the identification of damage location directly. It is the combination of various mode shapes, $\widetilde{W}_n'''(x) \cdot \widetilde{W}_n(x) - \widetilde{W}_n''(x) \cdot \widetilde{W}_n'(x)$, that changes with the damage locally. Therefore, a damage index based on the modal power flow can be defined as

$$\beta_{P_n}(x) = \frac{\widetilde{P}_n(x)/\tilde{\omega}_n \widetilde{D}_E}{\max \mid \widetilde{P}_n(x)/\tilde{\omega}_n \widetilde{D}_E \mid} = \frac{\widetilde{W}_n'''(x) \cdot \widetilde{W}_n(x) - \widetilde{W}_n''(x) \cdot \widetilde{W}_n'(x)}{\max\{\widetilde{W}_n'''(x) \cdot \tilde{W}_n(x) - \widetilde{W}_n''(x) \cdot \widetilde{W}_n'(x)\}} \tag{28}$$

Compared with an arbitrary combination of a mode shape and its derivatives, the damage index defined by Eq. (28) has definite and clear physical meaning, that is, it represents energy distribution along the structure for a given mode shape. Since any damage will induce a local change of energy, it is expected that the proposed damage index is sensitive to various damages and would have higher sensitivity.

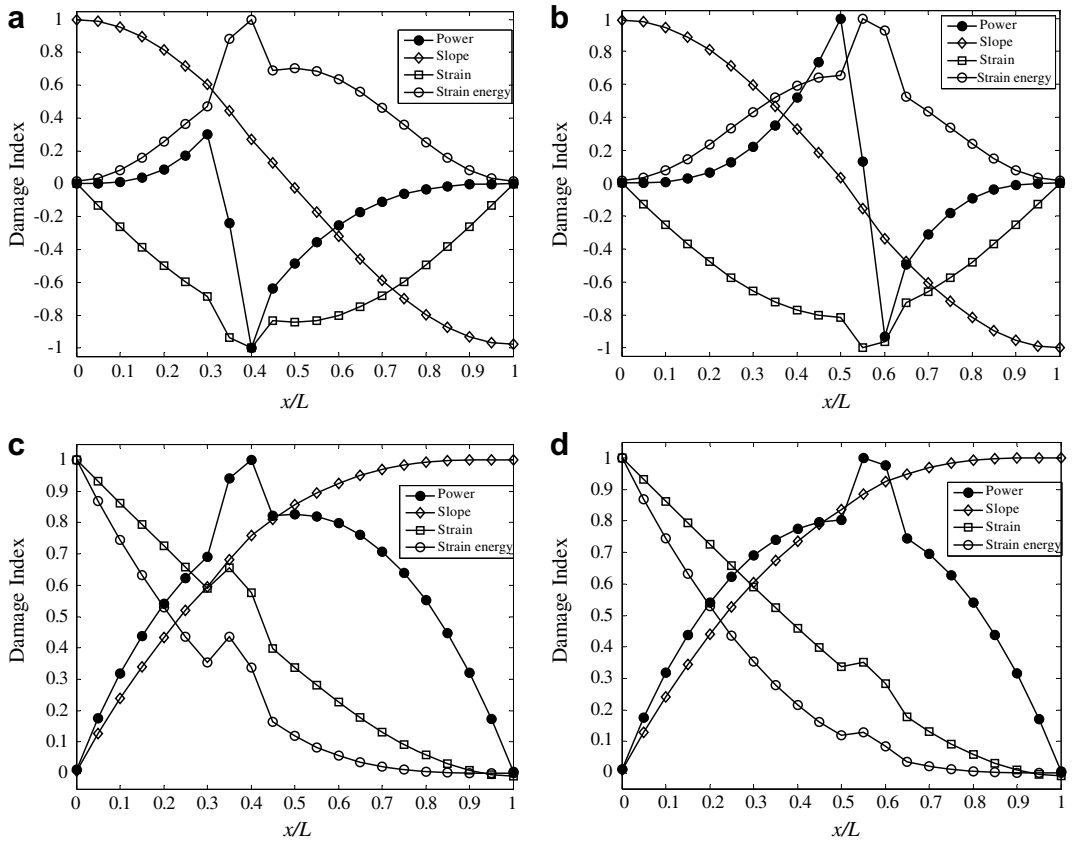

Fig. 4. Comparison of various damage indices for the delaminated beam with different boundary conditions and damage locations. The length of delaminated region is $\Delta x_d = 0.1$ L. (a) Simply-supported beam, $x_d/L = 0.3$; (b) simply-supported beam, $x_d/L = 0.5$ and (c) cantilever beam, $x_d/L = 0.3$; (d) cantilever beam, $x_d/L = 0.5$.

4.2. Numerical examples

Numerical examples are presented to compare the proposed damage index, β_{P_n}, with the damage indices based on the slope, the bending strain, as well as the strain energy associated with the mode. For the bending strain, the damage index proposed by Li et al. [17] is used, written as

$$\beta_{\varepsilon_n}(x) = \frac{\widetilde{W}''_n(x)}{\max \mid \widetilde{W}''_n(x) \mid}. \tag{29}$$

For the slope and the strain energy of the mode, similar damage indices can be defined as

$$\beta_{\phi_n}(x) = \frac{\widetilde{W}'_n(x)}{\max \mid \widetilde{W}'_n(x) \mid}, \quad \text{and} \tag{30a}$$

$$\beta_{E_n}(x) = \frac{\tilde{W}''^2_n(x)}{\max \mid \tilde{W}''^2_n(x) \mid}. \tag{30b}$$

In the examples, the intact beam is assumed to be uniform with a span of length $L = 1$ m and rectangular cross section, as shown in Fig. 3a. The height and the width of the beam are $h = 0.1$ m and $b = 0.05$ m, respectively. The density and Young's modulus of beam material are assumed to be $\rho = 7800$ kg/m^3, and $E = 200$ GPa, respectively. In order to study the performance of the proposed damage index for a beam with imperfect boundary conditions, the beam is assumed to be elastically supported at each end by a translational spring and a rotational spring, whose spring constants are denoted by K_L, T_L, K_R, and T_R, the subscripts 'L' and 'R' representing the left and the right ends, respectively. Classical boundary conditions can be regarded as special cases of this general boundary condition. In Table 1 are listed the boundary conditions considered in the examples. Considering easy implementation in practical measurements, only the first mode is used to calculate all the four damage indices in the present study.

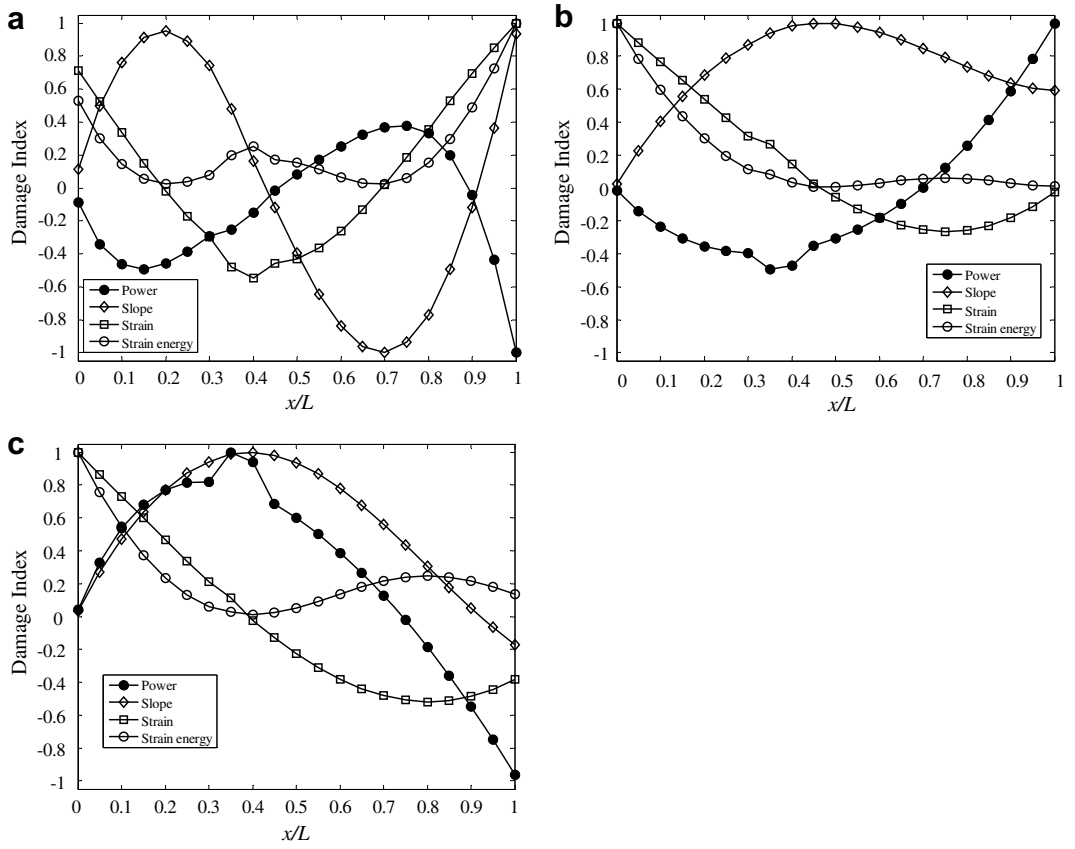

Fig. 5. Comparison of various damage indices for the delaminated beam with different elastic supports at the right-hand boundary. The crack is located at $x_d/L = 0.3$. $K_L = 10^{20}$, and $T_L = 10^{20}$. (a) $K_R = 10^{20}$, $T_R = 10^7$; (b) $K_R = 10^7$, $T_R = 10^{20}$ and (c) $K_R = 10^7$, $T_R = 10^7$.

4.2.1. A delaminated beam

Firstly, consider a delaminated beam as illustrated in Fig. 3b. The effect of delamination can be modeled by the reduction of bending stiffness *EI*. In the present example, a beam with a delaminated section of length $\Delta x_d/L = 0.1$ is considered. The damaged section is assumed to locate in $x/L = \{0.3, 0.4\}$ and $x/L = \{0.5, 0.6\}$, corresponding to $x_d = 0.3$ L and 0.5 L, respectively. The reduction of stiffness is taken to be 20%, that is, the bending stiffness in the damaged section is 80% of that for the intact beam.

A method developed by Chan and Wang [21] is used to calculate exact mode shapes of the beam, either intact or damaged, and the four damage indices are evaluated for comparison. The damaged beam is divided into three uniform beam sections, whose displacement functions are given by corresponding wave solutions, written as

$$W_{ni}(x) = A_{ni}\sin k_{ani}x + B_{ni}\cos k_{ani}x + C_{ni}\sinh k_{bni}x + D_{ni}\cosh k_{bni}x \tag{31}$$

where k_{ani} and k_{bni} are wave numbers associated with the propagating and the evanescent waves, respectively, $i = 1$, 2, and 3, representing the sections of $x = \{0, x_d\}$, $x = \{x_d, x_d + \Delta x_d\}$, and $x = \{x_d + \Delta x_d, L\}$, respectively.

At the two ends of the damaged section, the conditions of continuity are expressed as

$$W_{n1}(x_d) = W_{n2}(x_d), W'_{n1}(x_d) = W'_{n2}(x_d), \\ M_{n1}(x_d) = M_{n2}(x_d), Q_{n1}(x_d) = Q_{n2}(x_d) \tag{32a}$$

$$W_{n2}(x_d + \Delta x_d) = W_{n3}(x_d + \Delta x_d), W'_{n2}(x_d + \Delta x_d) = W'_{n3}(x_d + \Delta x_d), \\ M_{n2}(x_d + \Delta x_d) = M_{n3}(x_d + \Delta x_d), Q_{n2}(x_d + \Delta x_d) = Q_{n3}(x_d + \Delta x_d) \tag{32b}$$

Substituting Eq. (31) into Eqs. (32a) and (32b), one obtains

$$\{\mathbf{T}_{n1}\}\begin{pmatrix} A_{n1} \\ B_{n1} \\ C_{n1} \\ D_{n1} \end{pmatrix} = \{\mathbf{T}_{n2L}\}\begin{pmatrix} A_{n2} \\ B_{n2} \\ C_{n2} \\ D_{n2} \end{pmatrix}. \tag{33a}$$

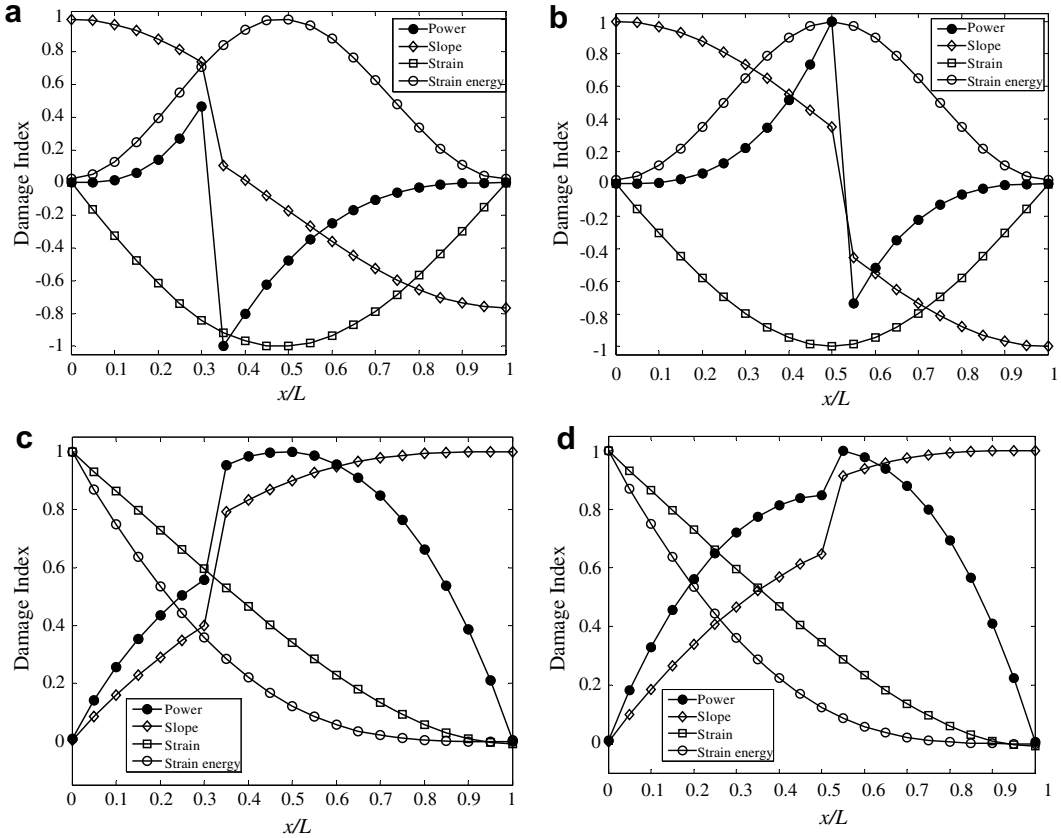

Fig. 6. Comparison of various damage indices for the cracked beam with different boundary conditions and damage locations. (a) Simply-supported beam, $x_d/L = 0.3$; (b) simply-supported beam, $x_d/L = 0.5$; (c) cantilever beam, $x_d/L = 0.3$; (d) cantilever beam, $x_d/L = 0.5$.

$$\{\mathbf{T}_{n2R}\}\begin{pmatrix} A_{n2} \\ B_{n2} \\ C_{n2} \\ D_{n2} \end{pmatrix} = \{\mathbf{T}_{n3}\}\begin{pmatrix} A_{n3} \\ B_{n3} \\ C_{n3} \\ D_{n3} \end{pmatrix}. \tag{33b}$$

In the example, a cantilever beam and a simply-supported beam are considered, and their boundary conditions can be written as

$$\{\mathbf{B}_{n1}\}\begin{pmatrix} A_{n1} \\ B_{n1} \\ C_{n1} \\ D_{n1} \end{pmatrix} = \begin{pmatrix} 0 \\ 0 \\ 0 \\ 0 \end{pmatrix}, \tag{34a}$$

$$\{\mathbf{B}_{n3}\}\begin{pmatrix} A_{n3} \\ B_{n3} \\ C_{n3} \\ D_{n3} \end{pmatrix} = \begin{pmatrix} 0 \\ 0 \\ 0 \\ 0 \end{pmatrix}. \tag{34b}$$

From Eqs. (33a), (33b) and (34a), (34b), the following eigenvalue problem is obtained

$$(\{\mathbf{B}_{n1}\} + \{\mathbf{B}_{n3}\}\{\mathbf{T}_{n3}\}^{-1}\{\mathbf{T}_{n2R}\}\{\mathbf{T}_{n2L}\}^{-1}\{\mathbf{T}_{n1}\})\begin{pmatrix} A_{n1} \\ B_{n1} \\ C_{n1} \\ D_{n1} \end{pmatrix} = \begin{pmatrix} 0 \\ 0 \\ 0 \\ 0 \end{pmatrix}, \tag{35}$$

whose solutions give the natural frequency and the coefficients $(A_{ni}\ B_{ni}\ C_{ni}\ D_{ni}), i = 1, 2, 3$. Once these coefficients and the wave numbers (calculated from the dispersion relation for given natural frequency) are known, the displacement mode

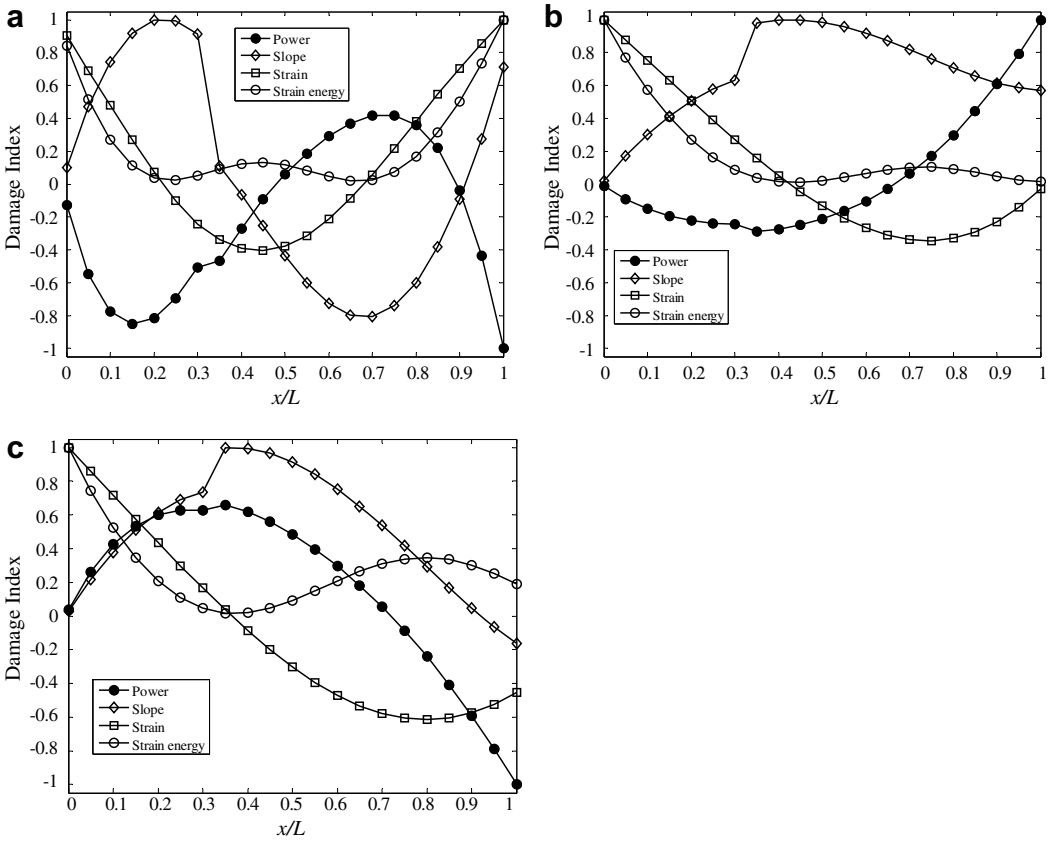

Fig. 7. Comparison of various damage indices for the cracked beam with different elastic supports at the right-hand boundary. The crack is located at $x_d/L = 0.3$. $K_L = 10^{20}$, and $T_L = 10^{20}$. (a) $K_R = 10^{20}$, $T_R = 10^7$; (b) $K_R = 10^7$, $T_R = 10^{20}$; (c) $K_R = 10^7$, $T_R = 10^7$.

shape and its derivatives are directly calculated rather than doing numerical differentiation. Afterwards, the four damage indices are evaluated using Eqs.(28)–(30), at 21 points uniformly distributed along the beam. This would give a picture similar to the result obtained from a practical measurement.

A comparison of the four damage indices for the delaminated beam with classical boundary conditions (cantilever and simply-supported) is shown in Fig. 4. It can be seen that the strain, the strain energy, and the power damage indices are sensitive to the delamination, while the slope damage index is not. Moreover, the sensitivity of the power damage index appears to be higher, especially for the simply-supported beam.

In Fig. 5 is shown the comparison for the beam with imperfect boundary supports. The damaged section is assumed to locate in $x/L = \{0.3, 0.4\}$. It can be seen that the power damage index is still sensitive to the damage, while the other damage indices are not. For the imperfect boundary support case shown in Fig. 5a, the sensitivity is low, suggesting that the boundary imperfection has a substantial effect in certain case.

4.2.2. A cracked beam

In the second example, a beam with a transverse crack at two locations, $x_d/L = 0.3$ and 0.5, is considered. For this case, the crack can be modeled by a rotational spring [22] as shown in Fig. 3c, whose elastic constant, T_c, is relevant to the depth of the crack. In the present example, the elastic constant is taken to be $T_c = 285D_E/L$. This value corresponds to a crack of depth of about 0.5 h.

The method developed by Chan and Wang [21] is also used to calculate the displacement mode shape of the cracked beam, which is modeled as two beam sections connected by the rotational spring. A cantilever beam and a simply-supported beam are considered.

A comparison of the four damage indices for the cracked beam with classical boundary conditions is shown in Fig. 6. For the crack-type damage, both the slope and the power damage indices are sensitive, whereas the strain and the strain energy damage indices are not. For the simply-supported beam, the sensitivity of the power damage index appears to be higher. For the cantilever beam, however, its sensitivity is similar to that of the slope damage index. In Fig. 7 is shown the comparison for the cracked beam with imperfect boundary supports. The crack is located at $x_d/L = 0.3$. The power damage index is still sensitive to the crack, although the slope damage index shows higher sensitivity. This suggests that a single damage indicator is usually not sufficient. A practical approach would be using a combination of selected damage indicators.

5. Conclusions

Features of power flow associated with vibration modes of an undamped finite beam are studied based on its fundamental definition using a higher-order beam theory. When the undamped beam undergoes free vibration at one of its natural frequencies, the reactive component of power flow is of modal behavior whose characteristic frequency is twice of the natural frequency, while the active component becomes zero. An energy analysis shows that the energy density associated with a vibration mode consists of a static component and a dynamic component, representing the mean total and Lagrangian energy densities, respectively. The spatial derivative of the modal power flow is proportional to the latter, but is independent of the former.

Potential application of the modal power flow to damage detection is studied. Two typical damages, the transverse crack and the delamination, are considered. A damage index based on the modal power flow is proposed. It is compared with the damage indices based on the slope, the strain, and the strain energy of the same mode through several numerical examples. A beam with elastic boundary supports is used in the examples so that the performance of the power damage index in the cases of imperfect boundary conditions can also be studied. It is shown that the damage index based on modal power flow is sensitive to both types of damage, even though the boundary supports are imperfect. This demonstrates the potential of the modal power flow as a universal damage indicator.

Acknowledgement

The third author wishes to acknowledge the support from a special fund for recently promoted Chair Professors given by The Hong Kong Polytechnic University.

References

[1] G. Pavic, Structure-borne energy flow, in: M.J. Crocker (Ed.), Encyclopedia of Acoustics, 1997, pp. 881–891.
[2] K.N. Mandal, S. Biswas, Shock Vib. Dig. 37 (2005) 3–11.
[3] L. Gavric, G. Pavic, J. Sound Vib. 164 (1993) 29–43.
[4] Y. Lace, M.N. Ichchou, L. Jezequel, J. Sound Vib. 192 (1996) 281–305.
[5] E.C.N. Wester, B.R. Mace, J. Sound Vib. 285 (2005) 209–227.
[6] D. Noiseux, J. Acoust. Soc. Am. 47 (1970) 238–247.
[7] G. Pavic, J. Sound Vib. 49 (1976) 221–230.
[8] B.R. Mace, C.R. Halkyard, L.H. El-Khatib, J. Sound Vib. 286 (2005) 507–527.
[9] J.-C. Pascal, J.-F. Li, X. Carniel, Shock Vib. 9 (2002) 57–66.
[10] A.E. Schwenk, S.D. Sommerfeldt, S.I. Hayek, J. Acoust. Soc. Am. 96 (1994) 2826–2835.
[11] P. Audrain, P. Masson, A. Berry, J. Acoust. Soc. Am. 108 (2000) 612–623.

[12] M.S. Khun, H.P. Lee, S.P. Lim, Struct. Eng. Mech. 16 (2003) 627–641.
[13] H.P. Lee, S.P. Lim, M.S. Khun, J. Sound Vib. 296 (2006) 602–622.
[14] X. Zhu, T.Y. Li, Y. Zhao, J.X. Liu, J. Sound Vib. 297 (2006) 215–226.
[15] X. Zhu, T.Y. Li, Y. Zhao, J. Yan, J. Sound Vib. 302 (2007) 332–349.
[16] A.K. Pandey, M. Biswas, M.M. Samman, J. Sound Vib. 145 (1991) 321–332.
[17] Y.Y. Li, L. Cheng, L.H. Yam, W.O. Wong, Comput. Struct. 80 (2002) 1881–1894.
[18] P. Cornwell, S.W. Doebling, C.R. Farrar, J. Sound Vib. 224 (1999) 359–374.
[19] S.W. Doebling, C.R. Farrar, M.B. Prime, D.W. Shevitz, Los Alamos National Laboratory report LA-13070-MS, 1996.
[20] H. Sohn, C.R. Farrar, F.M. Hemez, D.D. Shunk, D.W. Stinemates, B.R. Nadler, Los Alamos National Laboratory Report, LA-13976-MS, 2003.
[21] K.T. Chan, X.Q. Wang, J. Sound Vib. 206 (1997) 353–369.
[22] S.P. Lele, S.K. Maitl, J. Sound Vib. 257 (2002) 559–583.